

# Kinetics of Cryptdin-4 Translocation Coupled with Peptide-Induced Vesicle Leakage<sup>†</sup>

Jason E. Cummings and T. Kyle Vanderlick\*

Department of Chemical Engineering, Princeton University, Princeton, New Jersey 08544

Received June 5, 2007; Revised Manuscript Received August 23, 2007

**ABSTRACT:** The antimicrobial peptide cryptdin-4 (Crp4), a member of the  $\alpha$ -defensin family, is shown to translocate cooperatively across phospholipid bilayers. The cooperativity of the process is manifested by translocation kinetics which vary with the peptide to lipid molar ratio. A simple association model suggests dimerization. Black lipid membrane experiments reveal that Crp4 translocation does not create well-defined aqueous pores, as is often common among peptides exhibiting cooperative translocation. Still, the efflux induced by Crp4 upon its interaction with fluorophore-loaded vesicles is shown to be a direct result of the membrane perturbation resulting from the translocation process. Leakage can be predicted by relating membrane permeability to the fraction of peptide translocated. Crp4 translocation has implications for its antimicrobial activity as internalized peptide would be available to attack intracellular targets.

Antimicrobial peptides (AMPs)<sup>1</sup> are components of the innate immune system of their host organism and provide protection against a wide variety of pathogenic agents. Although small and relatively short (fewer than 50 amino acids), many AMPs display potent cidal activity toward bacteria, fungi, and viruses yet exhibit minimal toxicity against eukaryotic cells. While the exact mechanism of this cidal action remains uncertain, much evidence suggests that AMP-induced cell death is the result of membrane interaction and destabilization (1). Consequently, model membrane assays have become instrumental in understanding the mechanism of peptide binding and perturbation of biological membranes.

Two traits of AMPs, as affirmed by model membrane experiments, are critical to their ability to associate with the membrane lipids of pathogenic cells: net positive charge and amphiphilicity. Charge is important because the cationic nature of AMPs promotes selective interaction with the anionic membranes of many pathogens over the net neutral membranes of eukaryotic cells. Amphiphilicity allows the peptides to partition between the hydrophilic and hydrophobic regions of the membrane in a manner that disrupts membrane order and increases membrane permeability.

Vesicle leakage experiments provide a convenient and quantitative testing ground for studying peptide-induced perturbation of model membranes.

The mechanism of peptide-induced membrane perturbation varies from peptide to peptide. Some peptides are known to act cooperatively to form well-defined membrane pores spanning the width of the bilayer. Gramicidin, an  $\alpha$ -helical AMP, embodies this behavior as it dimerizes across a membrane and forms pores that can have lifetimes of several seconds (2). These pores are ion channels and allow leakage of encapsulated contents within lipid vesicles (3). The human neutrophil peptide HNP-2 works similarly (4). Other AMPs, such as magainin, melittin, and cryptdin-3, can also form membrane-spanning pores. Magainin and melittin initially lie parallel to the membrane, but upon oligomerization of four to six peptide molecules, they orient themselves perpendicular to the membrane, forming pores across the bilayer (5–9); the exact mechanism of cryptdin-3-induced pore formation is as yet undetermined, but data suggest that these membrane structures could be created by dimeric peptide complexes (10). Unlike gramicidin pores, however, the lifetime of pores created by magainin, melittin, and cryptdin-3 is only on the order of microseconds to tens of microseconds (7, 10). Despite this short existence, these transient structures still elicit substantial vesicle leakage.

Pore formation is not the only means via which membrane perturbation and vesicle leakage occur. Many peptides associate with membranes and induce leakage by creating ill-defined membrane defects. Dermaseptin S3 (DS3) and  $\delta$ -lysin are such examples. Both of these peptides assume  $\alpha$ -helices and exert their membrane disruptive activity by disordering the lipid packing while lying parallel to the membrane (11, 12). The mechanisms of these two peptides differ in that DS3 exercises its membrane activity in monomeric form while  $\delta$ -lysin acts as a trimer. Despite this difference, both peptides are potent membrane active agents.

<sup>†</sup> This work was supported by a fellowship to J.E.C. from the National Science Foundation.

\* To whom correspondence should be addressed. Phone: (609) 258-4891. Fax: (609) 258-0211. E-mail: vandertk@princeton.edu.

<sup>1</sup> Abbreviations: AMPs, antimicrobial peptides; Crp4, cryptdin-4; MLVs, multilamellar vesicles; LUVs, large unilamellar vesicles; POPG, 1-palmitoyl-2-oleoyl-*sn*-glycero-3-[phospho-*rac*-(1-glycerol)]; POPE, 1-palmitoyl-2-oleoyl-*sn*-glycero-3-phosphoethanolamine; DNS-PE, 1,2-dioleoyl-*sn*-glycero-3-phosphoethanolamine-*N*-(5-dimethylamino-1-naphthalenesulfonyl); NBD-PE, 1,2-dipalmitoyl-*sn*-glycero-3-phosphoethanolamine-*N*-(7-nitro-2-1,3-benzoxadiazol-4-yl); PEG2000-DPPE, 1,2-dipalmitoyl-*sn*-glycero-3-phosphoethanolamine-*N*-[methoxy(polyethylene glycol)-2000]; ANTS, 8-aminonaphthalene-1,3,6-trisulfonic acid; DPX, *p*-xylene-bis-pyridinium bromide; BLMs, black lipid membranes.

Peptide-induced membrane permeability allows redistribution of certain aqueous species, as well as membrane-bound species, across the barrier, including, in some instances, the peptide itself. In the cases of melittin and magainin, membrane pores are channels for peptide translocation (8, 9). The multimeric, short-lived pores created by those peptides allow a fraction of peptide molecules to redistribute to the vesicle membrane's inner monolayer upon pore disintegration. The balance of peptides remains bound to the outer monolayer.  $\delta$ -Lysin also translocates via a cooperative mechanism, but not through the formation of well-defined pores (12). In this case, a trio of peptides, oriented with their helices parallel to the membrane, diffuses as a unit through the membrane to reach the inner monolayer surface. Monomeric DS3 is an example of a peptide that does not, in practice, translocate (11).

Realizing the diversity of peptide action on lipid membranes, we feel it is important to elucidate the mechanism of peptide-induced membrane perturbation when studying the physical interactions of a membrane active peptide with lipid bilayers. In this work, we are concerned with an AMP found within the innate immune system of mice known as cryptdin-4 (Crp4). We investigate its interaction with lipid membranes, paying particular attention to its ability to translocate across the bilayer structures.

Crp4 is part of a large class of peptides known as  $\alpha$ -defensins.  $\alpha$ -Defensins are characterized by a  $\beta$ -sheet structure stiffened by three disulfide bonds and have been isolated from several organisms, including humans, rabbits, and mice (13). Crp4 is one peptide in a series of at least 17 homologous peptides existing in the small intestines of mice; these peptides are collectively termed cryptdins (14). Of the six peptides from that series that have been tested for bactericidal activity (i.e., Crp1–Crp6), Crp4 proved to be the most potent. This peptide is 32 amino acids long, has a molecular mass of  $\sim$ 3.8 kDa, and possesses a net charge of +8.5, properties not very different from those of its counterparts. Ouellette and co-workers at the University of California (Irvine, CA) have conducted numerous structure–activity studies on Crp4 with biological and model membrane assays to reveal the importance of specific residue identities, as well as the purpose of the  $\beta$ -sheet structure of the peptide (15–21). Although these studies have provided valuable information about the overall efficacy of Crp4 in inducing membrane perturbation and cell death, with respect to specific amino acid mutations, the finer mechanistic details of Crp4 action remain unclear. Here, we elucidate the translocation properties of Crp4 and show, with the use of a simple mathematical model, that translocation is responsible for the fluorophore efflux seen in vesicle leakage assays. We find that Crp4 translocation is a cooperative, non-pore-forming process.

Several assays have been developed for studying peptide translocation, each having pros and cons, and all generally used in a limited capacity where either the peptide concentration, lipid concentration, or both are held constant (6, 7, 9, 22, 23). Often assays are used only qualitatively to establish whether the peptide actually translocates. One assay relies upon enzyme digestion of peptide, as well as a concurrent FRET measurement between the tryptophan residue of the peptide and a fluorescently labeled lipid, to quantify the fraction of peptide that has translocated. For

this method to be useful, the peptide in question must of course be vulnerable to enzyme digestion and possess a tryptophan residue. A second assay employs fluorescently labeled multilamellar vesicles (MLVs) and an aqueous quencher that is impermeable to an unperturbed membrane, thereby initially quenching only those fluorophores in the outermost monolayer. Subjecting the MLVs to membrane active peptide allows quencher to permeate through the same number of bilayers as those that contain peptide. Thus, the degree of quenching reveals whether the peptide is translocating, but the method does not allow calculation of the fraction of peptide that translocates. A third assay, which eliminates some of the drawbacks of the previous two, is based solely on a FRET measurement between the Trp residue of the peptide and dansyl-labeled lipid. We not only use this assay in our study but also challenge its quantitative capabilities and verify that the molar ratio of membrane-bound peptide to lipid ( $P/L$ ) is the governing independent variable. This is important because absolute values of  $P$  and  $L$  have a marked effect on the fluorescence signals in the raw data (see Materials and Methods). Although only a small part of this work, confirming the robustness of this assay has strong practical utility.

## MATERIALS AND METHODS

**Peptide.** Cryptdin-4 (Crp4) and Trp-labeled cryptdin-4 (G1W-Crp4, the N-terminal glycine has been replaced with tryptophan) were purchased from New England Peptide, Inc. (Gardner, MA). The peptides were synthesized by solid phase peptide synthesis and were verified by HPLC and amino acid analysis. Both were  $>95\%$  pure. Explicit tests were not performed to determine if the folded structures of the peptides were correct. However, bactericidal assays and membrane leakage assays performed with these peptides and with Crp4 and G1W-Crp4 peptides from the research group of A. Ouellette at the Department of Pathology and Laboratory Medicine, University of California, showed identical results. The activities of the two Crp4 peptides were indistinguishable from each other as well as from the activities of the mutant peptides. Due to this consistency, and because the folded structure of the peptides from the Ouellette lab had been confirmed to be correct, we assumed that the purchased peptides were also folded correctly. Furthermore, we could also justify our use of G1W-Crp4 as an indicator of Crp4 activity.

**Lipids.** 1-Palmitoyl-2-oleoyl-*sn*-glycero-3-[phospho-*rac*-(1-glycerol)] (POPG), 1-palmitoyl-2-oleoyl-*sn*-glycero-3-phosphoethanolamine (POPE), 1,2-dioleoyl-*sn*-glycero-3-phosphoethanolamine-*N*-(5-dimethylamino-1-naphthalenesulfonyl) (DNS-PE), 1,2-dipalmitoyl-*sn*-glycero-3-phosphoethanolamine-*N*-(7-nitro-2-1,3-benzoxadiazol-4-yl) (NBD-PE), and 1,2-dipalmitoyl-*sn*-glycero-3-phosphoethanolamine-*N*-[methoxy(polyethylene glycol)-2000] (PEG2000-DPPE) were all purchased from Avanti Polar Lipids (Alabaster, AL).

The lipids used for this study were chosen for their prevalence in the membranes of bacterial cells. These membranes are often highly negatively charged due to a large presence of anionic lipids such as phosphatidylglycerol, cardiolipin, and phosphatidylserine (24). On the other hand, mammalian cell membranes are often enriched in zwitterionic

lipids such as phosphatidylcholine and phosphatidylethanolamine and are generally net neutral (24). Accordingly, the selection of lipids listed above allowed the creation of model membranes with lipid compositions closely resembling those of real bacterial membranes.

**Chemicals and Reagents.** 8-Aminonaphthalene-1,3,6-trisulfonic acid (ANTS) and *p*-xylene bis-pyridinium bromide (DPX) were purchased from Molecular Probes (Eugene, OR). Unless otherwise stated, all other chemicals were from Sigma-Aldrich (St. Louis, MO), of the highest grade available, and used as received. Water was produced by a Milli-Q UF unit (Millipore, Bedford, MA) and had a resistivity of 18.2 M $\Omega$ -cm.

**Preparation of Lipid Vesicles.** Large unilamellar vesicles (LUVs) were prepared by extruding (Lipex Biomembranes Inc.) dispersions of multilamellar vesicles (MLV) twice through a 400 nm polycarbonate filter (Nucleopore Co.), followed by 10 passes through a 100 nm polycarbonate filter. The MLV dispersions were formed by hydrating dried lipid films (3 mL of buffer) and subjecting them to five vortex–freeze–thaw cycles. Lipid concentrations were determined using a phosphorus assay explained in a procedure made available by Avanti Polar Lipids ([www.avantilipids.com](http://www.avantilipids.com)).

**Binding Assay.** POPG/PEG2000-DPPE (9.5:0.5) LUVs were prepared by hydrating a dried lipid film with an aqueous solution of 130 mM NaCl and 10 mM HEPES (260 mOsm/L, pH 7.4) and following the procedure outlined above (see Preparation of Lipid Vesicles). LUVs are titrated into a solution of G1W-Crp4 at a peptide concentration between 1 and 7  $\mu$ M. Binding is assessed by the intensity shift of the Trp fluorescence at 335 nm (excitation at 260 nm) as peptide partitions into the vesicle membrane. Trp spectra values are corrected to account for the effects of turbidity on fluorescence as proposed by Ladokhin et al., and the resulting data are fitted with a mole-fraction partition coefficient (25). We note that PEG2000-DPPE is used to prohibit the aggregation of lipid vesicles upon introduction into the peptide. The addition of this lipid, however, most likely does not interfere with peptide binding because the results of vesicle leakage assays (see below) with POPG LUVs and with POPG/PEG2000-DPPE LUVs subjected to Crp4 are identical.

**Translocation Assay Using Redistribution of the Fluorescent Peptide.** Fluorescently labeled LUVs were prepared by hydrating a POPG/PEG2000-DPPE/DNS-PE (8.5:0.5:1 molar ratio) lipid film with an aqueous solution of 130 mM NaCl and 10 mM HEPES (260 mOsm/L, pH 7.4) and following the procedure outlined above (see Preparation of Lipid Vesicles). Nonlabeled POPG/PEG2000-DPPE (9.5:0.5 molar ratio) LUVs were prepared similarly. PEG2000-DPPE was added to prevent aggregation and fusion of LUVs. Translocation was assessed by a fluorescence resonance energy transfer method using the membrane-bound DNS-PE and the Trp residue of G1W-Crp4 as described previously (9). In short, because of the peptide's high affinity for anionic membranes, RET causes the fluorescence of G1W-Crp4 (excitation at 280 nm, emission at 336 nm) to decrease significantly upon addition of DNS-PE-labeled vesicles to the peptide solution (Figure 1). Here, experiments were designed so that *P/L* ratios of 0.01, 0.02, and 0.03 were achieved after DNS-PE-labeled vesicles brought the lipid concentrations to 75, 150, and 225  $\mu$ M, respectively. After a predetermined incubation time, nonlabeled vesicles are

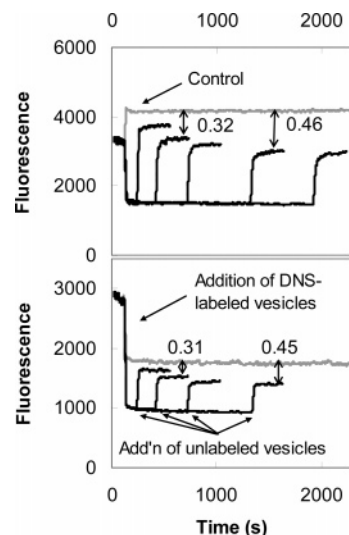


FIGURE 1: Translocation detected by Crp4 redistribution. The fluorescence intensity of Trp at 336 nm (excitation at 280 nm) was recorded as dansyl-labeled POPG vesicles were added to various concentrations of G1W-Crp4. Peptide binding to lipid is revealed as a sharp decrease in the fluorescence of the sample due to FRET. After a predetermined incubation time, an excess of nonlabeled POPG vesicles was added to the solution. Peptides redistribute between both sets of vesicles as shown by relief from FRET (i.e., an increase in fluorescence). The difference between the fluorescence intensity after the addition of nonlabeled vesicles (black lines) and the fluorescence intensity after simultaneous addition of both populations of vesicles (gray lines) reflects a fraction of translocated peptide. The top graph displays the raw fluorescence data at a peptide concentration of 1.5  $\mu$ M and a *P/L* of 0.02. The bottom graph displays the same data at a peptide concentration of 4.5  $\mu$ M and a *P/L* of 0.02. Although the fluorescence trends under the two conditions are clearly distinct, the fraction of peptide translocated is consistent, as shown by the numbers on the graph.

added in large excess (i.e., 9 times DNS-PE-labeled vesicles), and peptides redistribute between the two sets of vesicles. An increase in fluorescence results due to relief from RET. Those peptides that have translocated will not be immediately available for redistribution, and their fluorescence is still quenched. The difference in the fluorescence intensity of this sample and the fluorescence intensity of a sample where both vesicle populations were added at the same time reflects a fraction of translocated peptide. This fraction can be calculated according to the equation

$$\frac{(P_i/L)}{(P/L)} = \frac{F_{\text{control}} - F_{\text{redistribution}}}{F_{\text{control}} - F_{\text{quenched}}} \quad (1)$$

where the left-hand term is the fraction of peptide that has translocated,  $F_{\text{quenched}}$  is the fluorescence of the sample after addition of DNS-labeled vesicles,  $F_{\text{redistribution}}$  is the fluorescence of the sample after addition of unlabeled vesicles to a sample where DNS-labeled vesicles are already present, and  $F_{\text{control}}$  is the fluorescence of the sample after simultaneous addition of DNS-labeled and unlabeled vesicles. Derivation of eq 1 can be found in ref 9. It is important that quartz cuvettes be used for these experiments since the excitation and emission wavelengths are in the UV range.

Matsuzaki et al. (9) have confirmed the validity of values obtained with this assay by comparison with the values obtained with a direct measurement of peptide translocation. We note, however, that this assay is an indirect measurement

of peptide translocation and assumes that the peptide is able to redistribute across available external surfaces when new vesicles are added to the system; irreversible binding would lead to false analysis.

**Translocation Assay Using Dithionite Ion Permeability.** This assay relies on the use of fluorescently tagged multilamellar vesicles. These model membranes, composed of POPG and NBD-PE (9.95:0.05), were prepared as described previously (see Preparation of Lipid Vesicles). Translocation is determined by subjecting these MLVs to a 10 mM solution of the aqueous quencher sodium dithionite, both with and without peptide present as described previously (23); the dithionite cannot permeate through unperturbed lipid bilayers (i.e., those which do not incorporate any peptide). In the absence of peptide, sodium dithionite, which eliminates the fluorescence of NBD lipids (excitation at 450 nm, emission at 530 nm) by chemical reduction, quenches only those NBD groups in the outermost monolayer. This baseline degree of quenching establishes, in essence, the effective number of monolayers which compose the MLV. From this information, it is possible to infer if peptide infiltrates beyond the outermost (perturbed) monolayer as based on quenching data when both peptide and quencher are added to the vesicular solution. Such infiltration (if it occurs) is a direct signal of peptide translocation. Reported fluorescence values are normalized against the initial fluorescence in the absence of dithionite.

**Tryptophan Fluorescence Behavior and Translocation Assay Robustness.** Because we have performed our translocation experiments at various  $P/L$  values and various concentrations of lipid, it is important to offer background information about the behavior of Trp fluorescence to explain the raw data (Figure 1). It is well-recognized that the peak of the fluorescence spectrum of Trp shifts in both spectral position and intensity depending upon the polarity of the environment (i.e., hydrophilic vs hydrophobic) in which the residue exists (25). Because an additional intensity modulation can result from changes in sample turbidity as a consequence of the introduction of lipid vesicles, the fluorescence intensity at a given wavelength may increase or decrease depending on the absolute concentrations of peptide and lipid employed. Despite this apparent inconsistent behavior of Trp fluorescence, Figure 1 exhibits the robustness of the translocation assay and shows that accurate and repeatable results can be attained with this assay regardless of total peptide and lipid concentration.

**Measurement of Conductance on Black Lipid Membranes.** Solvent-free membranes were prepared as described by Montal and Mueller (26). Bilayer membranes were formed from a mixture of POPE and POPG (1:1 and 1:3) in pentane. BLMs were bathed in 130 mM NaCl, 10 mM HEPES, and 4.5 mM NaOH (pH 7.4). Two symmetrical halves of a Teflon chamber with solution volumes of 1.5 mL were divided by a 15  $\mu\text{m}$  thick Teflon partition containing a round aperture  $\sim 50 \mu\text{m}$  in diameter. Hexadecane in pentane (1:10, v/v) was used for the aperture pretreatment. Conductance measurements were performed using an Axopatch 200B amplifier (Axon Instruments) in the voltage clamp mode. The amplifier output signal was filtered by a low-pass eight-pole Butterworth filter (model 9002, Frequency Devices) at 15 kHz and directly saved into the computer memory with a sampling frequency of 50 kHz. Statistical analysis was performed using

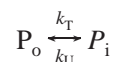
Clampfit 9.2 (Axon Instruments) as well as software developed in-house. A pair of Ag–AgCl electrodes in 2 M KCl bridges was used. “Virtual ground” was maintained at the trans side of the bilayer. Positive currents are therefore those of cations flowing from cis to trans. Bilayer formation was indicated by the subsequent increase in membrane capacitance to its final value of 80–100 pF. Measuring the bilayer’s conductance checked their stability. For unmodified bilayers, a conductance value of  $\sim 1$  pS was found, which remained unchanged for several hours. Crp4 was added to the aqueous phase at one (cis) side of the bilayer from stock solutions (1 mg/mL), and membrane conductance changes were measured subsequently. All experiments were performed at room temperature. Details on membrane preparation and the conductance measurements may be found elsewhere (27).

**Fluorescence-Based Vesicle Leakage Assays.** Crp4 was tested for its ability to induce leakage from large unilamellar phospholipid vesicles (LUVs) of defined composition. POPG LUVs were loaded with a fluorophore/quencher (ANTS/DPX) system under quenched conditions (28). Dried lipid films were hydrated with aqueous solutions consisting of 17 mM ANTS, 60.5 mM DPX, 10 mM HEPES, 31 mM NaCl, and 19.5 mM NaOH (260 mOsm/L, pH 7.4) and subjected to the procedure described above (see Preparation of Lipid Vesicles). Vesicles were separated from the unencapsulated ANTS/DPX system by gel-permeation chromatography with 130 mM NaCl, 10 mM HEPES, and 4.5 mM NaOH (260 mOsm/L, pH 7.4) as the column eluant. Vesicular suspensions diluted with eluant buffer to 75, 150, or 225  $\mu\text{M}$  total lipid were incubated with peptide at ambient temperature and at  $P/L$  values between 0 and 0.05. Time-dependent fluorescence produced by ANTS release was monitored at 520 nm (excitation at 353 nm). Fluorescence values were expressed relative to fluorescence obtained by vesicular solubilization with Triton X-100. Because the values obtained by this method of fluorescence normalization are not necessarily identical to the fraction of ANTS released, normalized fluorescence values were converted into actual fractions of ANTS released using the method of Ladokhin et al. (29, 30). This transformation altered fractional values by 2–5%.

## MODELING TRANSLOCATION

Translocation assays such as the one used in this study have, to the best of our knowledge, been previously used simply to verify the occurrence of peptide translocation. As the issue of cooperativity is a key feature of many translocation mechanisms, we show here that translocation assays can be used more broadly in this context by examining the kinetics of translocation. In particular, the simple models below reveal that cooperativity in translocation is associated with a kinetic response that depends on  $P/L$ .

First, we model the simplest case of noncooperative translocation of peptide across a membrane. This can be represented by



where  $P_o$  is the peptide bound to the outer monolayer of the membrane while  $P_i$  is the peptide bound to the inner

monolayer.  $k_T$  and  $k_U$  represent the forward and backward rate constants for translocation, respectively. Assuming all peptide in the system,  $P$ , is bound to the membrane,  $L$ , then  $P_o/L + P_i/L = P/L$ . Assuming further that  $k_T$  and  $k_U$  are equal, the translocation process follows this simple rate expression:

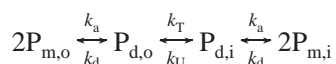
$$\frac{d\left(\frac{P_i}{L}\right)}{dt} = \frac{k_T}{P/L} \left( \frac{P}{L} - 2\frac{P_i}{L} \right) \quad (2)$$

Integration of this equation with the boundary condition that no peptide is present initially on the inner monolayer (i.e.,  $P_i/L = 0$  at  $t = 0$ ) leads to an expression for the fraction of peptide translocated:

$$\frac{P_i/L}{P/L} = \frac{1}{2}(1 - e^{-2k_T t}) \quad (3)$$

As one can clearly see, the kinetics of translocation are controlled only by the magnitude of the fundamental rate constant  $k_T$  and not by the magnitude of  $P/L$ . This is the hallmark of a noncooperative process.

If translocation involves cooperativity (i.e., oligomerization), we now show that  $P/L$  will affect the kinetic response by appealing to the simplest case of cooperativity, namely dimerization. This translocation scenario can be represented by



where  $P_{m,o}$  and  $P_{m,i}$  are the peptides that exist as monomers on the outer and inner monolayers, respectively, while the peptides that exist as dimers are denoted by  $P_{d,o}$  and  $P_{d,i}$ , respectively. The rate constant for the association of two monomers to form a dimer is given by  $k_a$ , while  $k_d$  is the corresponding dissociation constant. The system of equations corresponding to this simple cooperative translocation scheme is given by

$$\frac{d(P_{m,o}/L)}{dt} = -2k_a(P_{m,o}/L)^2 + 2k_d(P_{d,o}/L) \quad (4)$$

$$\frac{d(P_{d,o}/L)}{dt} = k_a(P_{m,o}/L)^2 - k_d(P_{d,o}/L) - k_T(P_{d,o}/L) + k_U(P_{d,i}/L) \quad (5)$$

$$\frac{d(P_{d,i}/L)}{dt} = k_T(P_{d,o}/L) - k_U(P_{d,i}/L) - k_d(P_{d,i}/L) + k_a(P_{m,i}/L)^2 \quad (6)$$

$$P_{m,i}/L = P/L - P_{m,o}/L - 2(P_{d,o}/L) - 2(P_{d,i}/L) \quad (7)$$

This system can be simplified by invoking a local equilibrium assumption where the dimerization step occurs much faster than the translocation step. The system of equations then simplifies to

$$\frac{d(P_{d,i}/L)}{dt} = k_T \left( \frac{P_{d,o}}{L} - \frac{P_{d,i}}{L} \right) \quad (8)$$

$$(P_{m,i}/L) = P/L - P_{m,o}/L - 2(P_{d,o}/L) - 2(P_{d,i}/L) \quad (9)$$

$$K_{\text{assoc}} = \frac{(P_{d,o}/L)}{(P_{m,o}/L)^2} = \frac{(P_{d,i}/L)}{(P_{m,i}/L)^2} \quad (10)$$

where  $K_{\text{assoc}}$  is the equilibrium constant for the dimerization step, and we have again assumed that  $k_T = k_U$ . We note that equating  $k_T$  and  $k_U$  means that the equilibrium fraction of translocated peptide is 0.5. Equations 8–10 can now be combined to form a single rate equation for the fraction of peptide translocated:

$$\frac{d\left(\frac{P_i}{L}\right)}{dt} = \frac{k_T}{P/L} \left( \frac{P}{L} - 2\frac{P_i}{L} \right) + \frac{k_T}{P/L} \frac{1}{4K_{\text{assoc}}} \left\{ \left( 1 + 8K_{\text{assoc}} \frac{P_i}{L} \right)^{1/2} - \left[ 1 + 8K_{\text{assoc}} \left( \frac{P}{L} - \frac{P_i}{L} \right) \right]^{1/2} \right\} \quad (11)$$

where  $P_i/L$  is the molar ratio of peptide to lipid on the inner monolayer. This rate equation clearly reveals that  $P/L$  plays a role in determining translocation kinetics, a property not seen in the noncooperative model. In fact, the cooperativity is embodied in the second term on the right-hand side of this expression. This term is always negative and serves to slow the rate as compared to the noncooperative process, which is embodied in the first term on the right-hand side. Essentially, cooperativity necessitates additional time for peptide aggregation to occur, the importance of which decreases as  $P/L$  increases due to the higher probability of peptides finding one another (or equivalently, cooperativity decreases the fraction of peptide available to translocate).

Finally, we note that, in the context of this simple model, if  $K_{\text{assoc}}$  is small, then the dynamics of translocation are driven by the product of  $k_T$  and  $K_{\text{assoc}}$  (which can be shown using a Taylor series expansion to the second order). Thus, in this limit, model fits to experimental data cannot yield independent estimates of  $k_T$  and  $K_{\text{assoc}}$ .

## RESULTS

**Peptide Binding.** A small but important point is to establish the binding affinity of the positively charged Crp4 for the negatively charged POPG membranes used in this study. Ideally, the translocation and leakage assays are best performed under conditions where peptide is fully bound. Indeed, the translocation model presented above assumes this situation.

The extent of peptide binding in our experiments can be established by referring to Figure 2 which shows the corrected fluorescence response (see Materials and Methods) of Trp as POPG vesicles are titrated into a solution of G1W-Crp4. As one can readily see, as the amount of lipid in the system,  $L$ , is increased, the driving force for peptide adsorption also increases, leading asymptotically to conditions corresponding to the fully bound state. Using a model proposed by Ladokhin et al. and as shown by the dashed line in Figure 2, this data can be fitted to yield a mole-fraction partition coefficient of  $2.7 \times 10^7$  (25). This value indicates that >90% of total peptide is bound to membrane at the  $P/L$  values used in our translocation and leakage assays (i.e.,  $P/L \leq 0.05$ ). In the regime of nearly complete binding,  $P/L$ , and not the individual value of peptide or lipid concentration,

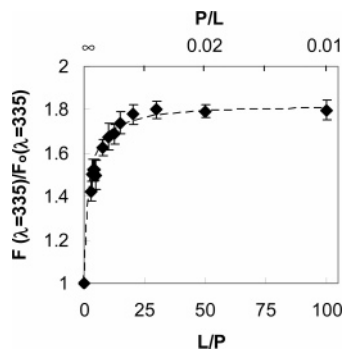


FIGURE 2: Binding affinity of Crp4 for POPG vesicles. Trp-labeled Crp4 at concentrations between 1 and 7  $\mu\text{M}$  was titrated with POPG/PEG2000-DPPE (9.5:0.5) LUVs. As the peptide partitions between the aqueous phase and the lipid phase, the fluorescence spectra of the Trp residue shift in both spectral position and intensity due to a change in the polarity of the environment and turbidity of the solution. Here the fluorescence at 335 nm is monitored with lipid addition and normalized against the fluorescence of the sample at 335 nm when no lipid is present, with appropriate corrections made to the fluorescence values to account for changes in sample turbidity. The dashed line through the data is the best fit line, according to a model proposed by Ladokhin et al., yielding a mole-fraction partition coefficient of  $\sim 2.7 \times 10^7$  (25).

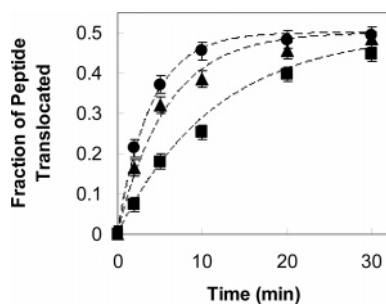


FIGURE 3: Kinetics of Crp4 translocation. G1W-Crp4 samples at concentrations between 0.75 and 6.75  $\mu\text{M}$  were mixed with dansyl-labeled POPG vesicles to bring the  $P/L$  to 0.01 (■), 0.02 (▲), and 0.03 (●). Each data point is an average of six independent measurements. The translocation of Crp4 is time-dependent and displays distinct kinetics for the three values of  $P/L$ , behavior which is suggestive of a cooperative translocation process. The lines through the data are best overall fit lines using a dimerization model where the same fitting parameters are maintained for each  $P/L$  value. The total peptide concentration has no effect on the time scale for translocation.

should be the controlling parameter. To verify this, assays were performed at the same  $P/L$  values for various lipid concentrations.

**Translocation.** The translocation of peptide across vesicle membranes can be assessed using the FRET mechanism between the Trp residue of G1W-Crp4 and DNS-PE (see Materials and Methods). In Figure 3, the kinetics of G1W-Crp4 translocation are plotted for  $P/L$  values of 0.01, 0.02, and 0.03. Every point in the figure is an average value obtained at three different total lipid concentrations: 75, 150, and 225  $\mu\text{M}$ . The lack of dependence on absolute concentrations verifies that the molar ratio of membrane-bound peptide to lipid ( $P/L$ ) is the governing independent variable. As one can readily see, all data sets appear to have an asymptote of 0.5, while the kinetics of translocation become faster with an increase in  $P/L$ . The distinct kinetic responses of translocation for various  $P/L$  values suggest some degree of peptide oligomerization (see Modeling Translocation). The lines in the figure correspond to theoretical fits using the

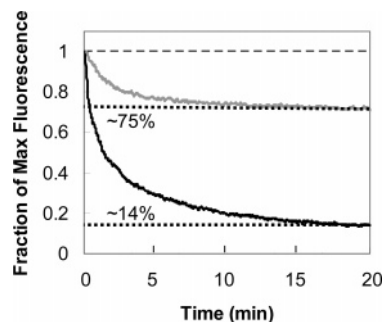


FIGURE 4: Translocation detected by the membrane permeability of sodium dithionite. POPG/NBD-PE (9.95:0.05) MLVs were added to a solution of sodium dithionite only (gray line) or to a solution of sodium dithionite and Crp4 (black line). Dithionite, which cannot permeate through unperturbed lipid bilayers, irreversibly quenches NBD fluorescence. In the absence of peptide, dithionite quenches only those NBD groups in the outermost monolayer ( $\sim 25\%$  of total NBD groups). In the presence of peptide, the level of quenching exceeds 85%, suggesting that Crp4 translocates across the outermost bilayer and attacks the first inner bilayer.

simple dimerization model presented above. Least-squares analysis was used to determine a single value for  $k_T$  and a single value for  $K_{\text{assoc}}$  so the entire data set could be best fit. Fitting analysis reveals that  $K_{\text{assoc}} < 1$ . As discussed earlier, in the limit of low  $K_{\text{assoc}}$ , the kinetics of translocation are determined by the product of  $K_{\text{assoc}}$  and  $k_T$ . Consequently, several combinations of values for  $k_T$  and  $K_{\text{assoc}}$  fit the data equally well, so it is not possible to extract specific values for these parameters (beyond the finding that  $K_{\text{assoc}}$  is small). The key point, however, is that the different kinetic responses (as a function of  $P/L$ ) are adequately represented by this simple model.

As stated previously (Materials and Methods), the translocation assay used above may lead to a false positive (i.e., that translocation occurs) if the peptide is unable to redistribute itself between vesicle exteriors (due to irreversible binding). Thus, to confirm the occurrence of translocation of Crp4, we have conducted a second, albeit qualitative, test of peptide translocation using the sodium dithionite permeability assay mentioned in the introductory section. As shown by the gray line in Figure 4, addition of membrane-impermeable sodium dithionite to MLVs of POPG and NBD-PE (9.95:0.05) quenches the fluorophores residing in the outermost monolayer of the vesicles (i.e., 25% of the initial NBD fluorescence). If addition of Crp4 results in perturbation of simply the outer monolayer of the MLV, thereby permitting the quencher to access only as far as the first interlamellar space, the maximum quenching that could occur would be 75%. However, as shown by the black line in Figure 4, addition of dithionite to MLVs in the presence of Crp4 allows the quencher to access more than 85% of the NBD groups. This suggests that Crp4 is able to translocate across the outermost bilayer of the MLV and then attack the first inner bilayer.

**Black Lipid Membrane (BLM) Experiments.** The presence of oligomers introduces the question of whether translocation proceeds through well-defined membrane pores. The creation of such structures by surface active peptides can be revealed by measuring the electrical properties of a lipid membrane in the presence of peptide. In these experiments, a planar bilayer separates two aqueous solutions and resists the flow of electrical current between the apposed electrolytic fluids.

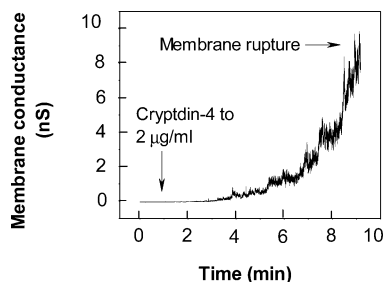


FIGURE 5: Effect of Crp4 on membrane conductance. Crp4 was applied to one side of a planar bilayer formed from a 1:1 mixture of POPG and POPE. Exposure of membrane to peptide led to a developing increase in membrane conductance and eventual membrane rupture. Typically, the creation of distinct membrane pores is manifested by repeating stepwise conductance events. However, none were observed in experiments with Crp4.

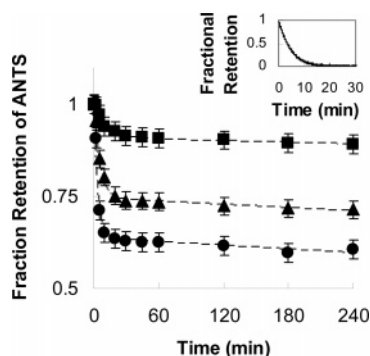


FIGURE 6: Kinetics of Crp4-induced vesicle leakage. Crp4 at concentrations between 0.75 and 6.75  $\mu\text{M}$  was incubated with fluorophore-loaded POPG vesicles as the fluorescence of the samples was collected at regular intervals for 4 h.  $P/L$  was brought to 0.01 (■), 0.02 (▲), and 0.03 (●) with addition of lipid and is the sole variable affecting the kinetics and magnitude of leakage; the total peptide concentration has no effect on the leakage behavior. Leakage is largely due to the translocation of Crp4, resulting in a biphasic kinetic leakage response. The lines through the data are best fit lines according to the leakage model defined by eqs 12 and 13, where the fitting parameters  $D_1$  and  $D_2$  are adjusted according to a least-squares analysis. The inset is a depiction of surfactant-induced leakage where the kinetics follow an exponential decay to zero.

The bilayer resistance can be calculated by invoking a known voltage across the membrane and applying Ohm's law. The formation of distinct aqueous membrane channels is manifested by the appearance of reproducible stepwise conductance events. This type of behavior was not observed in our BLM experiments. Our results show a developing increase in membrane conductance and eventual membrane rupture for a 50:50 POPG/POPE bilayer (Figure 5). Similar results were obtained for a 75:25 POPG/POPE bilayer (data not shown). This evidence demonstrates that Crp4 under the experimental conditions that were chosen does not form well-defined membrane pores.

**Vesicle Leakage.** Vesicle leakage was monitored by measuring changes in the fluorescence intensity of the sample as fluorophore escaped the interior of POPG vesicles after addition of Crp4 (see Materials and Methods). Figure 6 plots the fractional retention within vesicles versus time for each  $P/L$  tested and reveals an initial rapid release of contents followed by a very slow but steady residual leakage. As  $P/L$  increases, the kinetics of release, as well as the extent of leakage at any given time, also increase. Each  $P/L$  data set

shown within Figure 6 is an average of data gathered at three different total lipid concentrations (i.e., 75, 150, and 225  $\mu\text{M}$ ); again, it is clear that the operative independent variable is  $P/L$ . Notably, the time scale over which the major portion of leakage occurs is similar to the time scale for translocation. We propose to connect the two phenomena in the Discussion.

## DISCUSSION

We find that the translocation of Crp4 across lipid bilayers is a time-dependent, cooperative process occurring through ill-defined defects, where the molar ratio of peptide to lipid controls the time scale over which translocation occurs. Similarly, vesicle leakage elicited by Crp4 is also dictated by  $P/L$ , and the time scale for leakage very closely resembles that of translocation. Here, we intend to connect the two events. We first discuss details of the interaction of Crp4 with lipid membranes and show that translocation of this peptide is unexpected but explicable. We then present a leakage model to describe the vesicle leakage behavior induced by Crp4, using the translocation model presented above as input. Finally, we discuss the biological implications of Crp4 translocation for microbicidal activity.

Given the low content of hydrophobic residues existing within Crp4's primary structure ( $\sim 38\%$ ), penetration of this peptide into the membrane core and translocation across the membrane seem unlikely. In fact, Satchell and co-workers have used a novel colorimetric assay to show that Crp4, once bound, resides in a superficial position on the membrane, interacting primarily with the hydrophilic lipid headgroups (19, 31). Nevertheless, our data clearly demonstrate that Crp4 not only translocates but also employs some level of peptide cooperativity (i.e., dimerization or greater) to overcome the thermodynamic obstacle of crossing the membrane. In general, oligomerization can create peptide structures with a spatial arrangement of hydrophilic/hydrophobic regions that maximizes favorable interactions with the membrane. A cooperative translocation effort can explain how a largely hydrophilic peptide is able to move from the hydrophilic membrane periphery through the hydrophobic membrane interior.

The  $\alpha$ -helical peptides magainin and melittin are popular examples of peptides that use cooperative translocation mechanisms (8, 9). In their folded conformation, these peptides have distinct polar and nonpolar faces. Upon oligomerization, these peptides insert themselves into the membrane to create an aqueous pore with their hydrophilic regions lining the opening and their hydrophobic regions making contact with the membrane core. These pores are short-lived and are vehicles for peptide translocation. Likewise, some  $\beta$ -sheet peptides also contain segregated hydrophobic and hydrophilic regions that aid in their ability to move across a membrane in a cooperative fashion. The dimer-forming human defensins HNP-2 and HNP-3 are such examples (4).

NMR experiments with Crp4 have revealed its  $\beta$ -sheet structure and have shown that residues of opposite polarity (i.e., hydrophilic vs hydrophobic) are, to a large extent, segregated within the peptide structure (15). Although this scenario is not exclusive, one side of the peptide is highly nonpolar and the other side of the peptide contains the

majority of polar residues. Juxtaposed peptide molecules can likely position their similarly polarized surfaces to optimize peptide–peptide and peptide–membrane interactions facilitating translocation. This type of arrangement would necessitate the proximity of charged residues from adjacent Crp4 molecules and likely explains why our model predicts that  $K_{\text{assoc}}$  is a small number.

Peptide cooperativity in translocation often creates membrane defects with distinct boundaries and definite size. Wimley et al. report that HNP-2 dimers can associate with other HNP-2 dimers to form well-defined membrane pores as large as 25 Å (4). In the cases of magainin and melittin, peptides spawn well-defined pores on the order of 20–30 Å (6, 8). This behavior, however, does not hold true for Crp4. Despite the cooperativity exhibited by this peptide, BLM data suggest that such well-defined structures are not afforded by its translocation.

Although not well-defined, the defects created by the translocation of Crp4 can be identified as the source of vesicle leakage and are responsible for the initial rapid release of encapsulated vesicular contents seen in Figure 6. After crossing the membrane, Crp4 returns to the membrane periphery, as suggested by Satchell and co-workers, and is only minimally disruptive (19). This marginal membrane perturbation causes a residual leakage of encapsulated contents from the lipid vesicles at a level which still depends on  $P/L$ . We propose a simple model for leakage which is consistent with this mechanism and is able to predict the extent of leakage seen experimentally.

Our leakage model assumes that the only limitation to fluorophore transport is its diffusion across the membrane (i.e., no gradient in concentration of fluorophore exists inside or outside the vesicle). In this case, a simple mass balance on the concentration of encapsulated fluorophore yields

$$\frac{dC_i}{dt} = -\frac{3}{r_v d} D C_i \quad (12)$$

where  $C_i$  is the concentration of fluorophore inside the vesicles,  $t$  is time,  $r_v$  is the vesicle radius,  $d$  is the bilayer thickness, and  $D$  is the diffusion coefficient of the fluorescent molecules across the membrane. In addition, it is reasonable to assume that the concentration of fluorophore in the extravascular space is zero (we note that the total vesicular volume is less than 0.1% of the total sample volume). To test the validity of this basic transport scenario, we perform a simple experiment in which  $D$  is presumed to be constant and thus the kinetic efflux of the fluorophore should follow an exponential curve. This can be accomplished by monitoring leakage across vesicles laden with surfactants (32). As shown in the inset of Figure 6, this is exactly the behavior seen when fluorophore-loaded POPG vesicles are exposed to surfactant nonoxynol-9. As a benchmark value, we note that the time-independent diffusion coefficient is approximately  $6 \times 10^{-17}$  cm<sup>2</sup>/s.

Clearly, the kinetic efflux of fluorophore as induced by Crp4 (as shown in Figure 6) does not follow a simple exponential function (i.e.,  $D$  is not a constant). We assert that this behavior is a result of the translocation process where the kinetics of translocation control the instantaneous value of  $D$ . To map the kinetics of translocation onto the kinetics of leakage, we employ a simple affine transformation

relating the instantaneous diffusion coefficient to the fraction of peptide translocated at any given time:

$$\frac{D(t) - D_1}{D_2 - D_1} = \frac{0.5 - \frac{P_i/L}{P/L}}{0.5} \quad (13)$$

where  $D_1$  corresponds to the diffusion coefficient when the fraction of peptide translocated is 0.5 (i.e., at equilibrium) and  $D_2$  corresponds to the diffusion coefficient when the fraction of peptide translocated is 0 (i.e., immediately after binding of peptide to vesicles); specific values of  $D_1$  and  $D_2$  will depend on  $P/L$  and will be determined by a least-squares fit of model predictions to experimental leakage data. Physically,  $D_2$  applies to the leakage that is a direct result of Crp4 translocation, while  $D_1$  applies to the leakage resulting from the perturbation of the membrane while peptide rests in the peripheral region of the bilayer.

Using this simple mapping between the fluorophore diffusivity and the extent of translocation, the leakage of fluorophore follows the dashed lines shown in Figure 6, which describe the experimental data exceptionally well. At a  $P/L$  of 0.01, the model predicts that  $D_2$  is  $1 \times 10^{-16}$  cm<sup>2</sup>/s and  $D_1$  is  $1 \times 10^{-18}$  cm<sup>2</sup>/s. Both these values increase with an increase in  $P/L$ .  $D_2$  displays a power dependence on  $P/L$  of  $\sim 2.4$  which may be reflective of the cooperative (i.e., dimeric) nature of the translocation process.  $D_1$ , on the other hand, is practically linear with  $P/L$ . This dependence may be an indication that Crp4 perturbs membranes as a monomer when resting in the superficial region of the bilayer. The relatively large value of  $D_2$ , as compared to  $D_1$ , emphasizes that the majority of membrane perturbation and vesicle leakage induced by Crp4 is due to the translocation process.

It is worthwhile to create a predictive model relating the extent of leakage to the independent variable  $P/L$ . To do so requires relationships between the diffusivity limits ( $D_1$  and  $D_2$ ) and  $P/L$ . At the simplest level,  $D_1$  can be ignored since its value at any substantial  $P/L$  is insignificant when compared with  $D_2$ . For  $D_2$ , we use the power law dependence given above and a value for the prefactor,  $\alpha$ , which best fits the data at the three  $P/L$  values that were examined. The resulting model is given by

$$\frac{dC_i}{dt} = -\frac{6}{r_v d} \alpha \left(\frac{P}{L}\right)^n C_i \left[0.5 - \left(\frac{P_i/L}{P/L}\right)(t)\right] \quad (14)$$

where  $n$  is 2.4 and  $\alpha$  is  $5.23 \times 10^4$ . We use this model to predict the leakage behavior of vesicles across an extended range of  $P/L$  values up to 0.05. In particular, we compare the fraction of contents leaked after 4 h to model predictions; by this point in time (see Figure 6), the vesicles have released virtually all that they will. As shown in Figure 7, the agreement is excellent and clearly demonstrates that Crp4 translocation is, in fact, responsible for the bulk of vesicle leakage induced by the peptide.

Although the lipid vesicles utilized for this study are essentially one-component systems (i.e., composed almost entirely of POPG), real bacterial membranes are highly complex matrices constructed of several lipid types (24). These various lipids can often phase separate within the membrane to form lipid domains containing a disproportionately high concentration of one or two particular lipids.

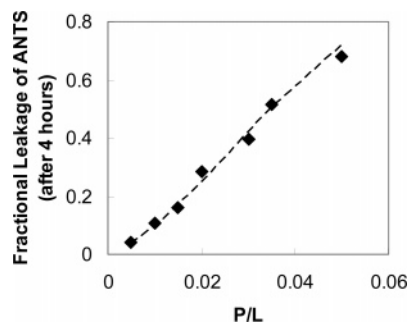


FIGURE 7: Crp4-induced vesicle leakage after 4 h. Crp4 was incubated with fluorophore-loaded POPG vesicles at  $P/L$  ratios of up to 0.05. An increase in sample fluorescence occurred as a result of peptide-induced membrane perturbation and subsequent fluorophore leakage. Fluorescence values were expressed relative to the fluorescence obtained by vesicular solubilization with Triton X-100 and converted into actual fractional leakage of ANTS according to a method proposed by Ladokhin et al. (29, 30). The line through the data shows the theoretical leakage given by the predictive leakage model (eq 14).

For example, *Escherichia coli* has been shown to contain a large number of domains enriched in cardiolipin (CL), which is essentially a dimer of the anionic lipid phosphatidylglycerol (PG) (33). Therefore, because Crp4 is known to have a high affinity for anionic lipids and virtually no attraction for zwitterionic lipids (34), the translocation of Crp4 across bacterial membranes may occur preferentially inside these negatively charged lipid domains.

Ramifications of Crp4 translocation extend beyond that of just membrane perturbation. Although current data suggest that the cidal activity of Crp4 is a result of its harmful action on the pathogenic membrane (14–21), the discovery of Crp4 translocation presents the possibility that Crp4 is available to attack intracellular targets. This idea is even more credible when one realizes that the process of Crp4 internalization is an independent mechanism of the peptide and does not require endocytosis by a living cell.

## CONCLUSION

In this study, we investigated the translocation ability of the mouse defensin Crp4 and showed that a cooperative mechanism facilitates the movement of peptide across a vesicle membrane. We challenged the robustness of a popular fluorescence translocation assay at various independent concentrations of peptide and lipid and confirmed that the molar ratio of peptide to lipid is the sole determinant of translocation kinetics. A simple association model assuming dimerization of peptide fits the entire translocation data set exceptionally well. Although translocation proceeds cooperatively, BLM experiments revealed that this process does not create distinct, well-defined membrane pores. Despite that, translocation is still responsible for the efflux of encapsulated contents from fluorophore-loaded vesicles as shown by a kinetic leakage model. Collectively, the results of this study elucidate fundamental details of Crp4-induced membrane perturbation, thereby offering further insight into the mechanism of Crp4 microbicidal activity.

## ACKNOWLEDGMENT

We thank Sergey Bezrukov and Philip Gurnev of the National Institutes of Health for help in conducting BLM experiments.

## REFERENCES

- Lehrer, R. I., Barton, A., Daher, K. A., Harwig, S. S. L., Ganz, T., and Selsted, M. E. (1989) Interactions of human defensins with *Escherichia coli*. Mechanism of bactericidal activity, *J. Clin. Invest.* 84, 553–561.
- Ring, A., and Sandblom, J. (1988) Evaluation of surface tension and ion occupancy effects on gramicidin A channel lifetime, *Biophys. J.* 53, 541–548.
- Portlock, S. H., Clague, M. J., and Cherry, R. J. (1990) Leakage of internal markers from erythrocytes and lipid vesicles induced by melittin, gramicidin S and alamethicin: A comparative study, *Biochim. Biophys. Acta* 1030, 1–10.
- Wimley, W. C., Selsted, M. E., and White, S. H. (1994) Interactions between human defensins and lipid bilayers: Evidence for formation of multimeric pores, *Protein Sci.* 3, 1362–1373.
- Fattal, E., Nir, S., Parente, R. A., and Szoka, F. C., Jr. (1994) Pore-forming peptides induce rapid phospholipid flip-flop in membranes, *Biochemistry* 33, 6721–6731.
- Matsuzaki, K., Mitani, Y., Akada, K.-y., Murase, O., Yoneyama, S., Zasloff, M., and Miyajima, K. (1998) Mechanism of synergism between antimicrobial peptides magainin 2 and PGLa, *Biochemistry* 37, 15144–15153.
- Matsuzaki, K., Murase, O., and Miyajima, K. (1995) Kinetics of pore formation by an antimicrobial peptide, magainin 2, in phospholipid bilayers, *Biochemistry* 34, 12553–12559.
- Matsuzaki, K., Yoneyama, S., and Miyajima, K. (1997) Pore formation and translocation of melittin, *Biophys. J.* 73, 831–838.
- Matsuzaki, K., Murase, O., Fujii, N., and Miyajima, K. (1995) Translocation of a channel-forming antimicrobial peptide, magainin 2, across lipid bilayers by forming a pore, *Biochemistry* 34, 6521–6526.
- Yue, G., Merlin, D., Selsted, M. E., Lencer, W. I., Madara, J. L., and Eaton, D. C. (2002) Cryptdin 3 forms anion selective channels in cytoplasmic membranes of human embryonic kidney cells, *Am. J. Physiol.* 282, 757–765.
- Ghosh, J. K., Shaool, D., Guillaud, P., Ciceron, L., Mazier, D., Kustanovich, I., Shai, Y., and Mor, A. (1997) Selective cytotoxicity of dermaseptin S3 toward intraerythrocytic plasmodium falciparum and the underlying molecular basis, *J. Biol. Chem.* 272, 31609–31616.
- Pokorny, A., Birkbeck, T. H., and Almeida, F. F. (2002) Mechanism and kinetics of  $\delta$ -lysin interaction with phospholipid vesicles, *Biochemistry* 41, 11044–11056.
- Lehrer, R. I., Lichtenstein, A. K., and Ganz, T. (1993) Defensins: Antimicrobial and cytotoxic peptides of mammalian cells, *Annu. Rev. Immunol.* 11, 105–128.
- Ouellette, A. J., Hsieh, M. M., Nosek, M. T., Cano-Gauci, D. F., Huttner, K. M., Buick, R. N., and Selsted, M. E. (1994) Mouse paneth cell defensins: Primary structures and antibacterial activities of numerous cryptdin isoforms, *Infect. Immun.* 62, 5040–5047.
- Jing, W., Hunter, H. N., Tanabe, H., Ouellette, A. J., and Vogel, H. J. (2004) Solution structure of cryptdin-4, a mouse paneth cell  $\alpha$ -defensin, *Biochemistry* 43, 15759–15766.
- Maemoto, A., Qu, X., Rosengren, K. J., Tanabe, H., Henschen-Edman, A., Craik, D. J., and Ouellette, A. J. (2004) Functional analysis of the  $\alpha$ -defensin disulfide array in mouse cryptdin-4, *J. Biol. Chem.* 279, 44188–44196.
- Rosengren, K. J., Daly, N. L., Fornander, L. M., Jonsson, L. M. H., Shirafuji, Y., Qu, X., Vogel, H. J., Ouellette, A. J., and Craik, D. J. (2006) Structural and functional characterization of the conserved salt bridge in mammalian paneth cell  $\alpha$ -defensins: Solution structures of mouse cryptdin-4 and (E15D)-cryptdin-4, *J. Biol. Chem.* 281, 28068–28078.
- Satchell, D. P., Sheynis, T., Kolusheva, S., Cummings, J. E., Vanderlick, T. K., Jelinek, R., Selsted, M. E., and Ouellette, A. J. (2003) Quantitative interactions between cryptdin-4 amino terminal variants and membranes, *Peptides* 24, 1795–1805.
- Satchell, D. P., Sheynis, T., Shirafuji, Y., Kolusheva, S., Ouellette, A. J., and Jelinek, R. (2003) Interactions of mouse paneth cell  $\alpha$ -defensins and  $\alpha$ -defensin precursors with membranes, *J. Biol. Chem.* 278, 13838–13846.
- Tanabe, H., Qu, X., Weeks, C. S., Cummings, J. E., Kolusheva, S., Walsh, K. B., Jelinek, R., Vanderlick, T. K., and Ouellette, A. J. (2004) Structure-activity determinants in paneth cell  $\alpha$ -defensins: Loss-of-function in mouse cryptdin-4 by charge-

- reversal at arginine residue positions, *J. Biol. Chem.* 279, 11976–11983.
21. Weeks, C. S., Tanabe, H., Cummings, J. E., Crampton, S. P., Sheynis, T., Jelinek, R., Vanderlick, T. K., Cocco, M. J., and Ouellette, A. J. (2006) Matrix metalloproteinase-7 activation of mouse paneth cell pro- $\alpha$ -defensins: Ser43Ile44 proteolysis enables membrane-disruptive activity, *J. Biol. Chem.* 281, 28932–28942.
  22. Drin, G., and Tamsamani, J. (2002) Translocation of protegrin I through phospholipid membranes: Role of peptide folding, *Biochim. Biophys. Acta* 1559, 160–170.
  23. Matsuzaki, K., Yoneyama, S., Murase, O., and Miyajima, K. (1996) Transbilayer transport of ions and lipids coupled with mastoparan X translocation, *Biochemistry* 35, 8450–8456.
  24. Yeaman, M. R., and Yount, N. Y. (2003) Mechanisms of antimicrobial peptide action and resistance, *Pharmacol. Rev.* 55, 27–55.
  25. Ladokhin, A. S., Jayasinghe, S., and White, S. H. (2000) How to measure and analyze tryptophan fluorescence in membranes properly, and why bother? *Anal. Biochem.* 285, 235–245.
  26. Montal, M., and Mueller, P. (1972) Formation of bimolecular membranes from lipid monolayers and a study of their electrical properties, *Proc. Natl. Acad. Sci. U.S.A.* 69, 3561–3566.
  27. Bezrukov, S. M., and Vodyanoy, I. (1993) Probing alamethicin channels with water-soluble polymers. Effect on conductance of channel states, *Biophys. J.* 64, 16–25.
  28. Smolarsky, M., Teitelbaum, D., Sela, M., and Gitler, C. (1977) A simple fluorescent method to determine complement-mediated liposome immune lysis, *J. Immunol. Methods* 15, 255–265.
  29. Ladokhin, A. S., Wimley, W. C., Hristova, K., and White, S. H. (1997) Mechanism of leakage of contents of membrane vesicles determined by fluorescence reequenching, *Methods Enzymol.* 278, 474–486.
  30. Ladokhin, A. S., Wimley, W. C., and White, S. H. (1995) Leakage of membrane vesicle contents: Determination of mechanism using fluorescence reequenching, *Biophys. J.* 69, 1964–1971.
  31. Kolusheva, S., Shahal, T., and Jelinek, R. (2000) Peptide-membrane interactions studied by a new phospholipid/polydiacetylene colorimetric vesicle assay, *Biochemistry* 39, 15851–15859.
  32. Apel-Paz, M., Doncel, G. F., and Vanderlick, T. K. (2003) Membrane perturbation by surfactant candidates for STD prevention, *Langmuir* 19, 591–597.
  33. Mileykovskaya, E., and Dowhan, W. (2000) Visualization of phospholipid domains in *Escherichia coli* by using the cardiolipin-specific fluorescent dye 10-n-nonyl acridine orange, *J. Bacteriol.* 182, 1172–1175.
  34. Cummings, J. E., Satchell, D. P., Shirafuji, Y., Ouellette, A. J., and Vanderlick, T. K. (2003) Electrostatically controlled interactions of mouse paneth cell  $\alpha$ -defensins with phospholipid membranes, *Aust. J. Chem.* 56, 1031–1034.

BI701110M